Eur. Phys. J. A (2015) 51: 124
DOI 10.1140/epja/i2015-15124-x

THE EUROPEAN
PHYSICAL JOURNAL A

Regular Article – Theoretical Physics

Strange quark matter and strangelets in the improved quasiparticle model

Chen Wu[1,a] and Renli Xu[2,b]

[1] Shanghai Institute of Applied Physics, Chinese Academy of Sciences, Shanghai 201800, China
[2] Key Laboratory of Modern Acoustics and Department of Physics, Nanjing University, Nanjing 210093, China

Received: 15 June 2015 / Revised: 19 August 2015
Published online: 1 October 2015 –
Communicated by Xin-Nian Wang

Abstract. In this work, the properties of strange quark matter and strangelets are investigated within the framework of the improved quasiparticle model. The energy per baryon and particle chemical potentials as a function of the quark matter density are given. In particular, within the multiple reflection expansion method, the finite-size effects of strangelets are discussed in detail. The stable radius of a strangelet in the present model is smaller than, but comparable with that of the corresponding nucleus with the same baryon number. With the baryon number increment of stable strangelets, it is found that the surface tension decreases to $33\,\mathrm{MeV\,fm^{-2}}$ for strangelets with the baryon number greater than 10^4.

1 Introduction

Since the conjecture of Witten [1] that strange quark matter (SQM), rather than the normal nuclear matter, might be the true ground state of QCD, much theoretical and observational effort has been made on the investigation of its properties and potential astrophysical significance [2–4]. Meanwhile, searches for stable and metastable lumps of SQM, the so-called strangelets, are still an active area of nuclear physics research. SQM can exist in the inner core of dense strange stars. The collision of strange stars can release strangelets as an important part of cosmic rays [5,6]. Some of the cosmic-ray strangelets could be on the way to our Earth's atmosphere [7]. Terrestrially, the possible production of strangelets is studied in relativistic heavy-ion collisions [8]. In ref. [9], the STAR Collaboration claimed that they have achieved the sensitivity to the detection of the metastable strangelets with lifetime $\geq 0.1\,\mathrm{ns}$. Recently, we have studied the stability of the dibaryon ($\Xi^0\Xi^-$) within the framework of the quasiparticle model [10]. Our calculations showed that at least one weak decay channel opens for the dibaryon decay while all strong decay channels are closed. The results suggest the dibaryon ($\Xi^0\Xi^-$) is one of the favorable candidates for experimental detection.

Because of the well-known difficulty of QCD in the nonperturbative domain, many effective models reflecting the characteristics of the strong interaction are used to study SQM. One of the most famous models is the MIT bag model with which Farhi and Jaffe find that SQM is absolutely stable around the normal nuclear density for a wide range of parameters [2]. In the bag model, the quark mass is infinitely large outside while it is constant within the bag.

As is well known in nuclear physics, quark mass varies with environment. The effective mass has been extensively discussed, for example, within the Nambu-Jona-Lasinio (NJL) model [11] and within a quasiparticle model [12–18]. A chiral phase transition and dynamical symmetry breaking are demonstrated in the NJL model. In the literature, some authors have constructed the quasiparticle model in terms of the temperature- and density- dependent quark mass and made progress in studying the nonperturbative QCD model at finite density [12–15,19–22]. Since the quark mass depends on chemical potentials and temperature, the effective bag constant in these model is also a function of chemical potentials and temperature, in order to satisfy the fundamental relation of thermodynamics. Recently, the researchers have generalized a thermodynamic quasiparticle description of deconfined matter to finite chemical potential μ not yet accessible by present lattice calculations [23].

In this article, we study the properties of strange quark matter by using the improved quasiparticle model [23]. The energy per baryon and particle chemical potentials as a function of the quark matter density are described within the self-consistent thermodynamic treatment. Then we apply the improved quasiparticle model to study the properties of strangelets by including the important finite-size effect. It is found that the stable radius of

[a] e-mail: wuchenoffd@gmail.com
[b] e-mail: xurenli.phy@gmail.com

a strangelet is smaller than that of the corresponding ordinary nucleus with the same baryon number, which might be relevant for the analysis of the strangelet propagation and detection. Particularly, we present the finite-size effects of strangelets and calculate the surface energy and the surface tension *versus* the baryon number.

This paper is organized as follows. In sect. 2, we introduce the equation of state and formulate the improved quasiparticle model at finite chemical potential. The properties of strange quark matter are presented in sect. 3. Then in sect. 4, the improved quasiparticle model is extended to include the finite-size effect, and the properties of strangelets are calculated. Finally, a short summary is given in sect. 5.

2 The improved quasiparticle model

According to the improved quasiparticle model, the effective quark mass can be expressed as $m_i^2 = {m_{i0}}^2 + \Pi_i^*$, where m_{i0} and Π_i^* denote the rest mass and thermal mass of the quasiparticle, respectively. Π_i^* are given by the asymptotic values of the gauge-independent hard-thermal/density-loop self-energies [24]:

$$\Pi_i^* = 2\omega_{q0}(m_{i0}+\omega_{q0}),$$
$$\omega_{q0}^2 = \frac{N_c^2-1}{16N_c}\left(T^2+\frac{\mu_i^2}{\pi^2}\right)g^2, \qquad (1)$$

where μ_i denotes the quark chemical potential, and $N_c = 3$ is the number of colors. The thermodynamic potential density of a quasipartical system can be decomposed into the contributions of the quasiparticles and their mean field interaction B,

$$\Omega = \sum_i \Omega_i\left(T,\mu_i,m_i^2\right) + B(\Pi_i^*), \qquad (2)$$

where $\Omega_i = -d_i T\int \mathrm{d}^3k/(2\pi)^3 \ln(1+\exp\{(-\omega_i+\mu_i)/T\})$ are the contributions of the quarks (for the antiquarks, the chemical potential differs in the sign) and $d_i = 6$ count the degeneracy degrees of freedom. The function $B(\Pi_i^*)$ is determined from a thermodynamical self-consistency condition, via

$$\frac{\partial B}{\partial \Pi_i^*} = \frac{\partial \Omega_i(T,\mu_i,m_i^2)}{\partial m_i^2}, \qquad (3)$$

here $B = B_0 + B^*$ stands for the total bag constant, B_0 is regarded as a normal vacuum constant, and B^* is medium-dependent bag constant.

The entropy and the particle densities are given by the sum of the quasiparticle contributions as follows:

$$s_i = \frac{\partial \Omega_i(T,\mu_i,m_i^2)}{\partial T}, \qquad n_i = \frac{\partial \Omega_i(T,\mu_i,m_i^2)}{\partial \mu_i}. \qquad (4)$$

By comparison with lattice data at $\mu = 0$, Peshier *et al.* [24,25] have tested the quasiparticle approach, which can provide an appropriate description of the deconfined matter even close to the confinement transition, with the effective coupling in eq. (1) nonperturbatively parametrized by the following:

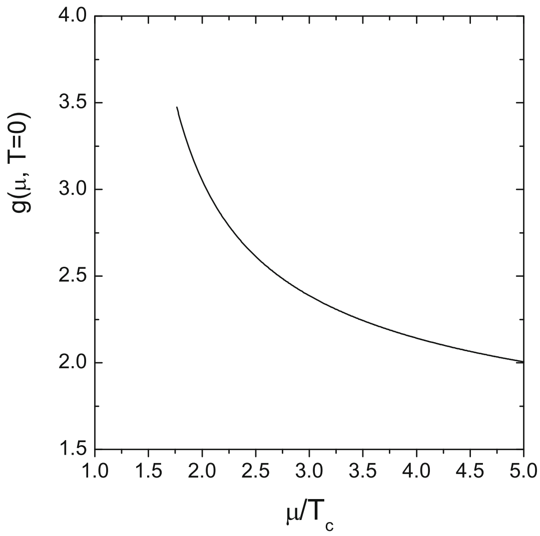

Fig. 1. The coupling constant $g(T = 0,\mu)$ as a function of μ.

$$g^2(T,\mu=0) = \frac{48\pi^2}{27\ln\left(\frac{T+T_s}{T_c/\lambda}\right)^2}, \qquad (5)$$

interpolating to the asymptotic limit of QCD.

Encouraged by the successful quasiparticle description of the $\mu = 0$ lattice data, the model has extrapolated to finite chemical potential. As a direct consequence, the Maxwell relation implies for the improved quasiparticle model

$$\sum_i\left[\frac{\partial n_i}{\partial m_i^2}\frac{\partial \Pi_i^*}{\partial T} - \frac{\partial s_i}{\partial m_i^2}\frac{\partial \Pi_i^*}{\partial \mu_i}\right] = 0, \qquad (6)$$

which is the integrability condition for the function B defined by eq. (3). Following directly from principles of thermodynamics, we can get a flow equation for the effective coupling with Π_i^* depending on g^2. This flow equation is quasilinear partial differential equation of the form

$$a_T\frac{\partial g^2}{\partial T} + a_\mu\frac{\partial g^2}{\partial \mu} = b, \qquad (7)$$

with the coefficients $a_{T,\mu}$ and b depending on T, μ, and g^2. Consequently, the running coupling in the asymptotic limit of large chemical potential can be simulated from that of large temperatures at zero chemical potential, which will help us to overcome the difficulty of calculating equation of state in nonperturbative regime [23].

Here we use the parameters $\lambda = 6.6$, $T_s = -0.78T_c$ and $T_C = 170\,\mathrm{MeV}$. For convenience later, we can approximately formulate $g(T = 0,\mu)$ as follows [26]:

$$g^2(T=0,\mu_i) = \frac{48\pi^2}{27\ln\left(\frac{\mu_i+T_s}{T_c\pi/\lambda}\right)^2}. \qquad (8)$$

The running coupling constant as a function of chemical potential $g(T = 0,\mu)$ is displayed in fig. 1. Based on the extended coupling constant, the equation of state of SQM is immediately obtained from the basic thermodynamic relations. In ref. [27], the authors utilized the improved quasiparticle model to obtain the equation of state and used it as an input to get the mass-radii relation of a pure quark star successfully.

In the present calculations we choose $m_{u0} = 5\,\text{MeV}$, $m_{d0} = 10\,\text{MeV}$ for up and down quarks [28], respectively. For the current mass of strange quarks, we take $m_{s0} = 120\,\text{MeV}$ which seems more reasonable according to the recent investigations of the current quark masses [28]. The adopted value of $B_0^{1/4} = 145\,\text{MeV}$ is equivalent to the conventional bag constant.

3 Bulk properties of deconfined strange quark matter

In this section we study the properties of SQM in bulk. As normally done, we assume SQM to be composed of u, d and s quarks and electrons. And weak equilibrium is always reached by the weak reactions such as

$$d, s \rightleftharpoons u + e + \bar{\nu}_e, \qquad s + u \rightleftharpoons u + d. \tag{9}$$

Correspondingly, relevant chemical potentials satisfy

$$\mu_d = \mu_s, \tag{10}$$

$$\mu_d = \mu_u + \mu_e. \tag{11}$$

There are only two independent chemical potentials from eqs. (10) and (11).

The condition of electric charge neutrality reads

$$\frac{2}{3}n_u - \frac{1}{3}n_d - \frac{1}{3}n_s - n_e = 0. \tag{12}$$

The baryon number density is defined as

$$n_B = \sum_{i=u,d,s} \frac{n_i}{3}\,. \tag{13}$$

We can calculate the two independent chemical potentials corresponding to a number density n_B by solving the two eqs. (12) and (13). Then we get the energy density and pressure from the thermodynamic potential density of quasipartical system in eq. (2).

In fig. 2, we show the energy per baryon as a function of the density. The minimum energy per baryon is larger than 930 MeV so that SQM is not absolutely stable in this improved quasiparticle model. The electric neutrality is enforced for bulk matter. The positive charge of quarks can be balanced by electrons. The chemical potentials of strange quarks and electrons *versus* the baryon number density are plotted in fig. 3. It can be seen that the chemical potential μ_e is in the range from 29 to 35 MeV, while the chemical potential μ_s increases with density increases. In fig. 4, we show the effective bag constant in eq. (3) as a function of the density. The effective bag constant increases at lower density and then decreases with the ascent of the density at higher density region. This is consistent with the fact that at extremely high densities, the quark confinement becomes less important.

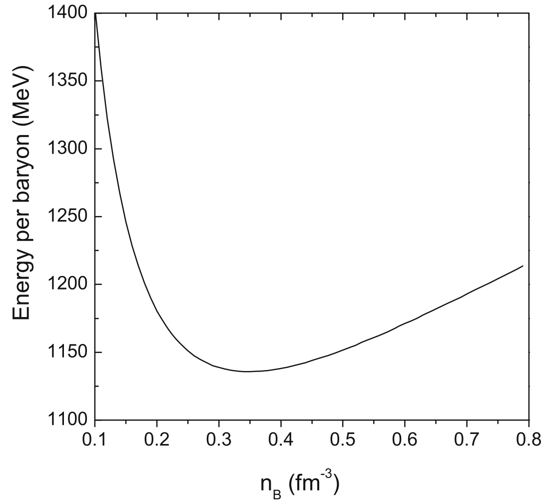

Fig. 2. The energy per baryon as a function of the density. The bag constant is $B_0^{1/4} = 145\,\text{MeV}$.

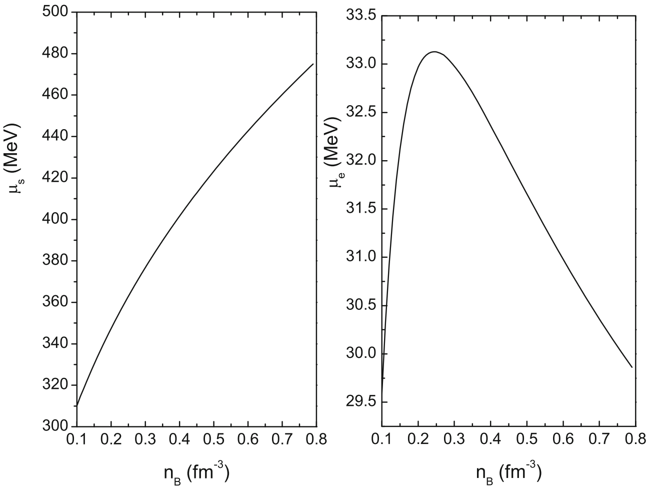

Fig. 3. The strange quark (left) and electron chemical potential (right) *versus* the density of quark matter. With increasing densities, the strange quark chemical potential increases. When the density is $0.25\,\text{fm}^{-3}$, the electron chemical potential approaches the maximum.

4 Properties of strangelet and finite-size effects

To study strangelets, it is necessary to extend the model to include finite-size effects. Although the mode-filling approach where the exact single-particle levels are filled one by one is good at finding the possible "stability island" [3], it becomes difficult when the baryon number is big. In this paper, we adopt the multi-reflection expansion approach where the system quantities are expanded to the negative-integer powers of the system radius [29,30].

The strangelet can be treated as an ideal gas of up, down and strange quarks, and the energy of this system is given by

$$E = \sum_i (\Omega_i + N_i\mu_i) + BV, \tag{14}$$

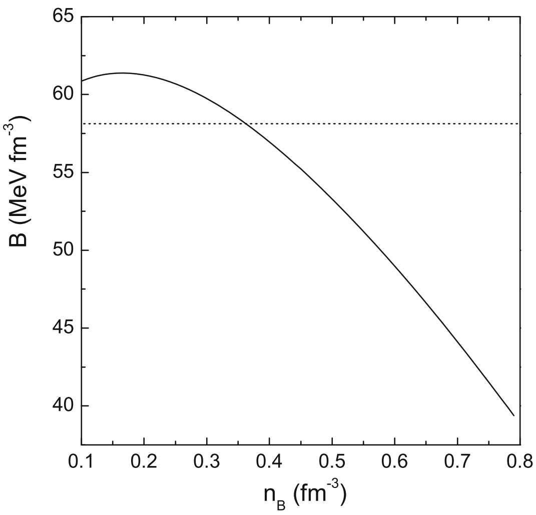

Fig. 4. The effective bag function B as a function of the density of strange quark matter. The horizontal line corresponds to the bag constant B_0.

here V stands for the bag volume, and N_i denote total number of quarks. The thermodynamical potential of quark species i can be written as

$$\Omega_i = \Omega_{i,V}V + \Omega_{i,S}S + \Omega_{i,C}C, \tag{15}$$

where $\partial\Omega_i/\partial\mu_i = -N_i$, the area $S = 4\pi R^2$, and the extrinsic curvature $C = 8\pi R$ for a sphere.

In a multiple reflection expansion theory [29,30] the thermodynamical quantities can be derived from a density of states of the form given by

$$\frac{\mathrm{d}N_i}{\mathrm{d}k} = 6\left[\frac{k^2V}{2\pi^2} + f_S^{(i)}\left(\frac{m_i}{k}\right)kS + f_C^{(i)}\left(\frac{m_i}{k}\right)C\right], \tag{16}$$

where the second term on the right-hand side of eq. (16) corresponding to the surface contribution was given by Berger and Jaffe [31] as

$$f_S^{(i)}\left(\frac{m_i}{k}\right) = -\frac{1}{8\pi}\left(1 - \frac{2}{\pi}\arctan\frac{k}{m}\right), \tag{17}$$

and the third term on the right-hand side of eq. (16) comes from curvature of the bag surface. Madsen [32] proposed the following ansatz for massive quarks:

$$f_C^{(i)}\left(\frac{m_i}{k}\right) = \frac{1}{12\pi^2}\left[1 - \frac{3k}{2m_i}\left(\frac{\pi}{2} - \arctan\frac{k}{m_i}\right)\right]. \tag{18}$$

The number density of each quark species can be obtained by means of

$$N_i = \int_0^{k_i^F} \frac{\mathrm{d}N_i}{\mathrm{d}k}\mathrm{d}k = n_{i,V}V + n_{i,S}S + n_{i,C}C, \tag{19}$$

with Fermi momentum $k_i^F = \sqrt{\mu_i^2 - m_i^2} = \mu_i(1 - \lambda_i^2)^{1/2}, \lambda_i \equiv m_i/\mu_i$.

The volume terms for quark species i are given by

$$\Omega_{i,V} = -\frac{\mu_i^4}{4\pi^2}\left((1-\lambda_i^2)^{1/2}\left(1 - \frac{5}{2}\lambda_i^2\right) + \frac{3}{2}\lambda_i^4 \ln\frac{1+(1-\lambda_i^2)^{1/2}}{\lambda_i}\right), \tag{20}$$

$$n_{i,V} = \frac{\mu_i^3}{\pi^2}(1-\lambda_i^2)^{3/2}. \tag{21}$$

The surface terms are given by

$$\Omega_{i,S} = \frac{3\mu_i^3}{4\pi}\left[\frac{1-\lambda_i^2}{6} - \frac{\lambda_i^2(1-\lambda_i)}{3} - \frac{1}{3\pi}\left(\arctan\frac{(1-\lambda_i^2)^{1/2}}{\lambda} - 2\lambda_i(1-\lambda_i^2)^{1/2} + \lambda_i^3\ln\frac{1+(1-\lambda_i^2)^{1/2}}{\lambda_i}\right)\right], \tag{22}$$

$$n_{i,S} = -\frac{3\mu_i^2}{4\pi}\left[\frac{1-\lambda_i^2}{2} - \frac{1}{\pi}\left(\arctan\frac{(1-\lambda_i^2)^{1/2}}{\lambda} - \lambda_i(1-\lambda_i^2)^{1/2}\right)\right]. \tag{23}$$

The curvature terms are given by

$$\Omega_{i,C} = \frac{\mu_i^2}{8\pi^2}\left[\lambda_i^2\ln\frac{1+(1-\lambda_i^2)^{1/2}}{\lambda_i} + \frac{\pi}{2\lambda_i} - \frac{3\pi\lambda_i}{2} + \pi\lambda_i^2 - \frac{1}{\lambda_i}\arctan\frac{(1-\lambda_i^2)^{1/2}}{\lambda_i}\right], \tag{24}$$

$$n_{i,C} = \frac{\mu_i}{8\pi^2}\left[(1-\lambda_i^2)^{1/2} - \frac{3\pi}{2}\frac{1-\lambda_i^2}{\lambda_i} + \frac{3}{\lambda_i}\arctan\frac{(1-\lambda_i^2)^{1/2}}{\lambda_i}\right]. \tag{25}$$

Once the thermodynamical potential is known, the energy density E can be obtained from eq. (14). In a strangelet, the weak equilibrium conditions, eqs. (10) and (11), are still valid due to the same reactions as in eq. (9). On the other hand, the strangelet size is generally much smaller than the Compton wavelength of electrons, and so electrons cannot be located within a strangelet. We therefore have $n_e = 0$. The total baryon number A of a strangelet can be expressed by

$$A = \frac{4}{3}\pi R^3 \frac{n_u + n_d + n_s}{3}. \tag{26}$$

For a given baryon number A, we can show the energy per baryon as a function of the radius, as in fig. 5, where $A = 100$ has been taken. The stable radius of the strangelet with baryon number $A = 100$ is about 4.3 fm. In the left graph of fig. 6, we show the energy per baryon *versus* the baryon number A up to 10^6, while the corresponding radius is plotted on the right graph of fig. 6. With increasing baryon number, the energy per baryon decreases while the radius increases. For the same baryon number, the radius of a strangelet is smaller than that of the corresponding ordinary nucleus, $R = 1.12A^{1/3}$ fm.

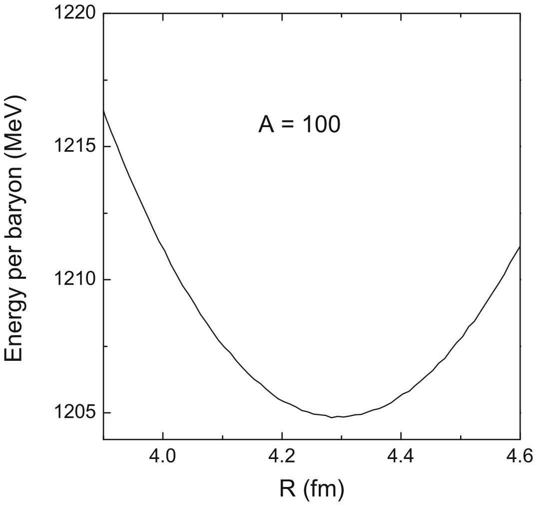

Fig. 5. The energy per baryon *versus* the radius of a strangelet with baryon number $A = 100$. The stable radius is about 4.3 fm.

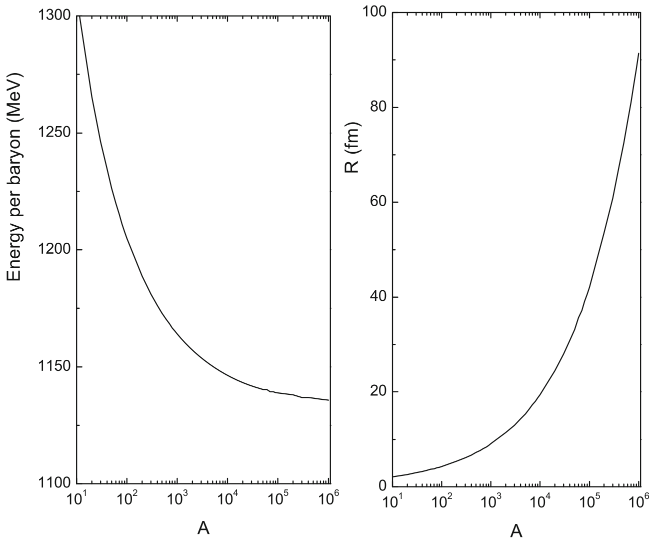

Fig. 6. The left graph denotes the energy per baryon as a function of the baryon number. The right graph denotes the radius of strangelets *versus* the baryon number.

It is well known that the surface tension is a fundamental parameter for the finite-size effects and nucleation phase transition [33]. The surface tension σ, the free energy per unit surface area can be defined as [34]

$$\sigma = \sum_i \frac{E_{S,i} V}{4\pi R^2} = \sum_i \frac{R}{3} \Omega_{S,i}. \tag{27}$$

In fig. 7, the surface energy per baryon is shown on the left graph and the total surface tension of strangelets is shown on the right graph. When the baryon number of strangelets increases to $A > 10^4$, the surface tension has a slight decline and comes gradually down to the vicinity of 33 MeV fm^{-2}, which is consistent with the range within 10–50 MeV fm^{-2} given by the pioneering work [35,36].

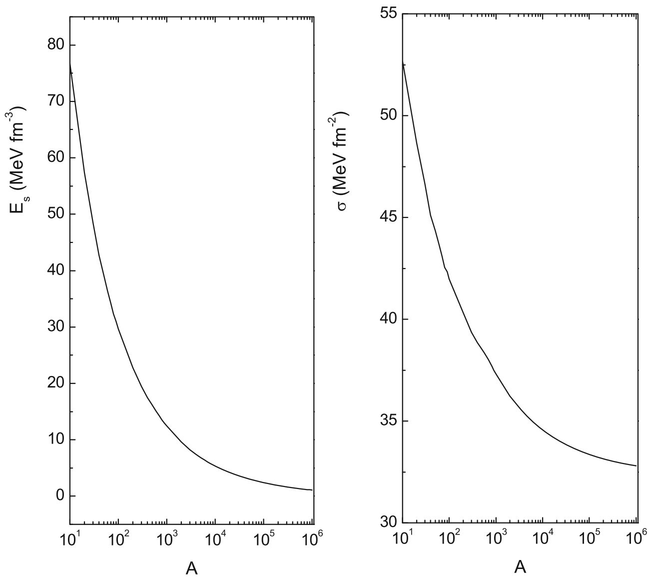

Fig. 7. The surface energies of strangelets are showed as a function of the baryon number A on the left graph. The right graph denotes the surface tension σ decreases with the increasing baryon number A.

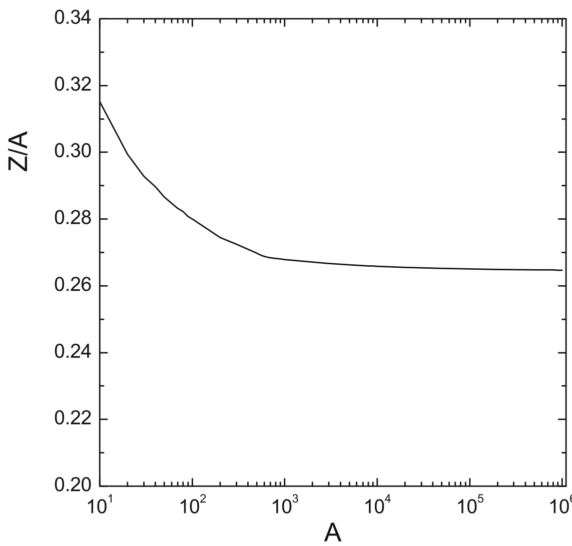

Fig. 8. The ratio Z/A of strangelets as a function of the baryon number A.

Finally, in fig. 8 we present the dependence of the electric charge for strangelets on the baryon number. When A is large, the behavior of Z as a function of A is $Z \simeq 0.265A$.

5 Summary

In summary, we have extended the quasiparticle model to include the finite-size effect and studied the properties of strange quark matter in bulk and strangelets. With the self-consistent thermodynamic treatment, the chemical potential-dependent effective bag constant and the equation of state of strange quark matter are calculated.

The properties of small strangelets have large dependence on the finite-size effect. By comparing the geometrical size of a strangelet with that of the corresponding ordinary nuclei, it is found that the strangelet radius is smaller than, but comparable with that of the ordinary nuclei with the same baryon number. The surface tension is approximately $33\,\mathrm{MeV\,fm^{-2}}$ in this model. SQM is not absolutely stable in this model, as explicitly presented in fig. 2. It is known that there are several methods to tackle the consistence of thermodynamical potential with the effective quark masses. Recently, The author Zong and his cooperators proposed mew thermodynamical treatment by using the partition function of a quasiparticle system [37,38]. Therefore, the stability of SQM needs to be further investigated in the future.

We thank Prof. Ru-Keng Su and Zhongzhou Ren for very helpful discussions. This work is supported partially by the Major State Basic Research Development Program in China (No. 2014CB845402).

References

1. E. Witten, Phys. Rev. D **30**, 272 (1984).
2. E. Farhi, R.L. Jaffe, Phys. Rev. D **30**, 2379 (1984).
3. E.P. Gilson, R.L. Jaffe, Phys. Rev. Lett. **71**, 332 (1993).
4. A.A. Isayev, Phys. Rev. C **91**, 015208 (2015).
5. S. Banerjee, S.K. Ghosh, S. Raha, D. Syam, Phys. Rev. Lett. **85**, 1384 (2000).
6. J. Madsen, Phys. Rev. D **71**, 014026 (2005).
7. B. Monreal, JHEP **02**, 077 (2007).
8. M. Weiner, Int. J. Mod. Phys. E **15**, 37 (2006).
9. STAR Collaboration, Phys. Rev. C **76**, 011901 (2007).
10. C. Wu, R. Xu, EPL **110**, 42001 (2015).
11. Y. Nambu, G. Jona-Lasinio, Phys. Rep. **122**, 345 (1961).
12. Y. Zhang, R.K. Su, S.Q. Ying, P. Wang, Europhys. Lett. **56**, 361 (2001).
13. X.J. Wen, J.Y. Li, J.Q. Liang, G.X. Peng, Phys. Rev. C **82**, 025809 (2010).
14. B.K. Patra, C.P. Singh, Phys. Rev. D **54**, 3551 (1996).
15. N. Prasad, C.P. Singh, Phys. Lett. B **501**, 92 (2001).
16. K. Schertler, C. Greiner, M.H. Thoma, Nucl. Phys. A **616**, 659 (1997).
17. M.I. Gorenstein, S.N. Yang, Phys. Rev. C **52**, 5206 (2001).
18. J.F. Xu, G.X. Peng, F. Liu, D.F. Hou, L.W. Chen, Phys. Rev. D **92**, 025025 (2015).
19. G.X. Peng, H.C. Chiang, P.Z. Ning, B.S. Zou, Phys. Rev. C **59**, 3542 (1999).
20. X.J. Wen, X.H. Zhong, G.X. Peng, P.N. Shen, P.Z. Ning, Phys. Rev. C **72**, 015204 (1999).
21. O.G. Benvenuto, G. Lugones, Phys. Rev. D **51**, 1987 (1995).
22. P. Wang, Phys. Rev. C **62**, 015204 (2000).
23. A. Peshier, B. Kämpfer, G. Soff, Phys. Rev. D **66**, 094003 (2002).
24. A. Peshier, B. Kämpfer, G. Soff, Phys. Phys. C **61**, 045203 (2000).
25. A. Peshier, B. Kampfer, G. Soff, arXiv:hep-ph/0106090v2.
26. X.P. Zheng, M. Kang, X.W. Liu, S.H. Yang, Phys. Rev. C **72**, 025809 (2005).
27. T. Zhao, Y. Yan, X.L. Luo, H.S. Zong, Phys. Rev. D **91**, 034018 (2015).
28. Particle Data Group (W.M. Yao *et al.*), J. Phys. G: Nucl. Part. Phys. **33**, 1 (2006).
29. R. Balian, C. Bloch, Ann. Phys. (N.Y.) **60**, 401 (1970).
30. T.H. Hanssan, R.L. Jaffe, Ann. Phys. (N.Y.) **151**, 204 (1983).
31. M.S. Berger, R.L. Jaffe, Phys. Rev. C **35**, 213 (1987) **44**, 566(E) (1991).
32. J. Madsen, Phys. Rev. D **47**, 5156 (1993).
33. S. Huang, J. Potvin, C. Rebbi, S. Sanielevici, Phys. Rev. D **42**, 2864 (1990).
34. B.C. Parija, Phys. Rev. C **48**, 2483 (1993).
35. H. Heiselberg, C.J. Pethick, E.F. Staubo, Phys. Rev. Lett. **70**, 1355 (1993).
36. K. Iida, K. Sato, Phys. Rev. C **58**, 2538 (1998).
37. L.J. Luo, J. Cao, Y. Yan, W.M. Sun, H.S. Zong, Eur. Phys. J. C **73**, 2626 (2013).
38. J. Cao, Y. Jiang, W.M. Sun, H.S. Zong, Phys. Lett. B **711**, 65 (2012).